Sustainable asphalt mixes manufactured with reclaimed asphalt and modified-lignin-stabilized bitumen emulsions

A. Yuliestyan[1], T. Gabet[2], P. Marsac[2], M. García-Morales[1], P. Partal[1*]

[1]*Departamento de Ingeniería Química, Centro de Investigación en Tecnología de Productos y Procesos Químicos (Pro²TecS), Campus de 'El Carmen', Universidad de Huelva, 21071, Huelva (Spain)*

[2]*IFSTTAR, MAST-MIT, F-44344Bougenais (France)*

[*]Author to whom correspondence should be addressed:

Dr. Pedro Partal López

E-mail: partal@uhu.es

Phone: +34 959 21 9989

Fax: +34 959 21 93 85

ABSTRACT

This work aims to develop asphalt mixes with 100 % reclaimed asphalt pavements (RAP) as source of aggregates and bitumen emulsions stabilized by amine-functionalized lignin. To that end, reduced-temperature asphalt technologies between 80 and 130 °C were assessed. Previously, processing parameters of emulsions were evaluated by droplet size distribution and rheology measurements. Furthermore, a study combining Pendant drop and Sessile drop (on a prototype polyethylene surface) tests showed that emulsion aqueous phase containing modified lignin would be able to wet the hydrophobic surface of RAP. Manufactured asphalt mixes were characterized according to French design method for hot mixes, including gyratory compaction, rutting resistance, complex modulus and fatigue resistance tests. The results obtained showed that reduced-temperature asphalt mixes could be successfully prepared to meet French design requirements, which would further minimize impact to environment. However, mix design has required a semi-quantitative approach for estimating 'active' RAP binder content, by balancing the manufacturing temperature and the fresh bitumen required.

Keywords: bitumen emulsion, lignin, rheology, reduced-temperature paving, product design.

1. INTRODUCTION

In the last decade, soaring pressure on the global environmental challenges demands immediate responses, as addressed in UN development agenda [1]. Particularly, issues involving sustainability, environment and economic aspects are mostly discussed. In transport infrastructure construction sector, an example for such issues is the use of fresh bituminous and aggregate material, which has a high impact, up to 40% of CO_{2eq} (defined as mass of CO_2 emitted in kg over a ton of each layer needed during the lifecycle), if the extraction and production process are considered within the boundaries of analysis [2]. Moreover, conventionally used hot mixes method during road construction may be perceived unsustainable due to its energetically unfavorable process and high CO_2 equivalent emitted to the air [3,4]. In that sense, a reduction of virgin material (bitumen and aggregates) and the use of reduced-temperature processes would promote more sustainable road designs, addressing both environmental and economic aspects.

Concerning the raw materials, the use of waste materials can be both economically and environmentally interesting due to the possible reduction of fresh binder, as well as the natural aggregates used [5]. Such example reports a lower down score by 15% in fossil depletion, when reclaimed asphalt pavement (RAP) was employed considering an impact assessment according to two sets of impact categories: midpoint (single issue) and end-point (higher aggregation level) categories, so called ReCiPe method [2]. That analysis is based on the comparison of three-structured layers (surface, binder and base) of which, one is manufactured with all virgin material and the other consist of up to 30% of RAP for the base layer. A reduction of 13-14 % in the cumulative energy demand has also been reported for 15% RAP recycled [6]. Besides those benefits, mechanical performance, stiffness modulus and rutting resistance could be improved [7–9]. Obviously, such utmost benefit may be expected for a higher RAP recycling rate. Today, their uses ,authorized in

Europe according to EN 13808-8 [10], are yet generally limited especially for surface layer [11]. This is related to the difficulty in controlling the characteristics of aged binder and aggregates that potentially affect recomposed asphalt mixes final performance. For that reason, many studies focus on studying the influence of incorporating RAP at higher percentage, even up to 100% recycling, on their mechanical behavior, aiming at speeding up its authorization [12].

Partial blending phenomena, between RAP binder and fresh bitumen, yet require understanding. This widely accepted concept results in altering the performance of blended binder [13,14]. For RAP recycling rate less than 25%, a study reports that no particular change in binder grade is necessary [15]. Another study suggests an increase of degree of partial blending from 70 to 96 % when mix compositions have been changed from involving 25% RAP and binder with PG 70-28 specification to 35% RAP and softer PG 50-28 [16]. From diffusion point of view in which diffusion coefficient and viscosity are related by Arrhenius function with temperature, the lower the viscosity of bitumen at a particular temperature (or softer characteristic), the more favorable the diffusion to occur due to high diffusion coefficient [17]. The comprehension of partial blending in HMA seems to drive in a converging direction, yet debatable on the investigation method for the moment. Unfortunately, when RAP is recomposed following a reduced-temperature mixing procedure, partial blending is another challenge. Many works done on recycled warm mixes mostly explain about bitumen content selection [8,18], with the assumption of fully recovered RAP binder and without partial blending. In this work, a semi-quantitative approach, referred to thin-film diffusion phenomenon, has been proposed trying to understand partial blending under reduced-temperature mixing conditions. As a result, the fraction of ‘active’ RAP binder blended with the fresh bitumen could be estimated.

Another interesting material that can potentially be used in road infrastructure is lignin. A study reports that lignin seems to be compatible with bitumen due to the similarity in their aromatic molecular structure [19]. Lignin is a renewable material, derived from wood in the form of lignocellulose. While the cellulose is the main input of pulp plant, lignin mainly ends up burnt in heat regenerator [20]. Due to the aromatic structure, lignin potential as a precursor for advanced materials could be opened through chemical modification. By lignin amination, for instance, cationic emulsifier for bitumen emulsion application could be obtained. Previous study [21] shows that modified lignin may prevent coalescence, as observed by insignificant change in average droplet size and its distribution profile, hence providing good stability. Despite stability during storage, bitumen emulsion also requires to wet the aggregate surface upon application, by a balance between the negative charge of the fresh aggregate and the positive charge of the cationic surfactant [22]. However, if the bitumen emulsion (and the emulsifier) is designed to coat a 100% RAP instead of virgin aggregates, its physical properties may not be treated equivalently due to the difference in surface characteristics. Thus, further research regarding emulsion/surfactant wettability on a hydrophobic surface is required to assess their interactions with RAP surface.

With the main objective to design asphalt mixes with maximum recycling and minimum impact to environment, this study is divided into three subtopics with the aims of: assessing the ability of emulsifiers derived from lignin to partially wet RAP surface; optimizing processing parameters during the manufacture of bitumen emulsion; and producing reduced-temperature asphalt mixes containing 100% RAP without sacrificing their mechanical performance.

2. EXPERIMENTAL

2.1. Materials

Kraft lignin (KL), tetra-ethylene-pentamine (TEPA) and formaldehyde, were used as reagents for producing cationic modified lignin (MKL). Kraft lignin used has a molecular weight of 10000 g/mol, an ash content of 3.14 wt.% and elemental composition (wt.%) consisting 61.15 of C, 6.72 of H, 26.92 of O, 2.18 of N and 2.54 of S. As for the reference, n-tallow alkyl tri-methylene diamine (referred to as REF), was selected. Penetration and Ring-and-Ball softening temperature tests were performed on bitumen according to EN 1426 and EN 1427 [23,24]. The values obtained were 190 dmm and 39 ºC, respectively. Reclaimed asphalt pavement material (RAP) was obtained from a real scale road fatigue simulator under accelerated heavy traffic, was kindly supplied by IFSTTAR (France).

2.2. Preparations

MKL emulsifier reaction procedure was presented elsewhere [21]. Afterwards, concentrated MKL was diluted with acidic water at pH 1 to attain final concentrations between 0.625 and 3.75%. Oil-in-water (O/W) emulsions were prepared by emulsifying 60 wt.% bitumen into that aqueous phase, at a selected concentration of 1.5 wt.% of MKL emulsifier. For sake of comparison, four emulsification devices were used in this study: A) three batch homogenizers UT T25, UT T50 and a SilL5M; and B) an inline three-stage high-shear homogenizer, referred to as 3STCM. The first three devices are small capacity processing units (200 – 500 gr). A premix of 145 °C bitumen and 60 °C of aqueous surfactant solution yielded a blend with an approximate temperature of 90 °C, to avoid water evaporation. Short after, emulsification at the maximum speed was done for 4 min. The difference with the in-line homogenizer type is in the capacity and the ability for continuous recirculation of the emulsion. When recirculation line was employed, the

maximum capacity is 5 kg, and emulsification time was further evaluated on 3STCM by taking sample through recirculating line starting from 1 to 12 minutes. For the reference emulsion stabilized by 0.5 wt.% REF, surfactant was dissolved in aqueous phase with pH 1 and the rest of procedures were similarly followed.

For RAP binder analysis, sample was extracted using perchloroethylene solvent on automatic asphalt analyser (EN 12697-1)[25] followed by binder recovery process in rotary evaporator (EN 12697-3)[26]. Details on the conditioning for mixing and compaction and the quantity of added water and fresh bitumen are presented in Table 1. The mixing was performed in two steps: first water addition for moisturizing RAP surface followed by bitumen emulsion addition for a total mixing time of 2.5 min. Compaction, apart from compaction study using gyratory compactor, was done using tire roller compactor. Once compacted, slabs were allowed for three days curing at 50 °C. For complex modulus and fatigues resistance tests, slabs were cut into trapezoidal specimen with sawing machine.

2.3. Tests and measurements

Surface tension measurements on acidic aqueous phase solution containing MKL emulsifier were done by the pendant drop method. The device consists of a camera with fixed focal length lense, pendant drop injector and LED lamp. The pendant drop was formed by a needle injector with outer diameter of 0.8 mm, and images were captured and analysed in real-time. Accurate surface tension measurements were obtained at the point that the drop was close to detach from the tip, when a more favorable deformation is caused by a bigger drop weight. With the same apparatus setup, the Sessile drop approach was used to test the contact angle between a polyethylene surface (used as reference hydrophobic prototype) and a drop of aqueous solution at varying

concentrations of the lignin surfactant studied. The procedure was adapted from general methodology explained elsewhere [27].

Bitumen emulsion properties were characterized by means of droplet size distribution (DSD) and viscous flow tests. DSD measurements were conducted in a laser diffraction analyzer, at ambient temperature. The refractive indices for bitumen and water were set at 1.61 and 1.33, respectively. Viscous flow tests at 30 °C were carried out in a controlled-stress rheometer, using a coaxial cylinder Z20-DIN (27 mm diameter) geometry, on steady rotational shear mode. Tests were performed by progressively increasing shear stress applied to obtain shear rate ranges between 0.1 and 500 s^{-1}. An equilibration time of 2 min was set at every stress applied, to achieve steady state conditions. Geometry used was serrated type for avoiding wall-slip phenomena. For binders, flow tests between 0.01 – 50 s^{-1} were performed on extracted RAP bitumen and fresh bitumen, using plate-plate geometry, at four temperatures of 60, 90, 120 and 150 °C.

Characterization of asphalt mixes was performed at four levels according to French design method [11]. In the first level, gyratory compactor was used to analyse their compaction behaviour. Loose mixes specimen was compacted in a rotating 150 mm diameter cylindrical mould with internal angle and vertical pressure settings according to EN 12697-31 Annex A [28]. The second level deals with rutting resistance that was done with the wheel tracking device, according to EN-12697-22 [29] for large size devices. Parallelepiped specimens of 100 mm thickness were subjected to alternating wheel/tire 5 kN load at a frequency of 1 Hz (inside chamber at 60 °C) for up to 30000 cycles. Afterward, complex modulus was measured in 2 points bending, according to EN-12697-26 Annex A [30]. A sinusoidal small deformation was applied on trapezoidal specimens for frequencies from 1 to 40 Hz, at each specified temperature between -10 and 40 °C. The last test (fourth level) is a fatigue test according to EN-12697-24 Annex A [30].

Trapezoidal specimens were subjected to a sinusoidal strain with constant amplitude between 80 and 150 μstrain in 2 points bending. The failure criterion is 50% reduction of the stiffness. Figure 1 summarized methodology followed for mix design.

3. RESULTS AND DISCUSSION

3.1. Surface activity of modified lignin emulsifier

As a preliminary attempt to foresee interfacial activity at the emulsion O/W interface and the expected wettability improvement caused by the surfactant, the polar and dispersive components of the surface tension of aqueous solutions containing increasing concentrations of the modified lignin (MKL) were determined. Calculations involved Sessile drop contact angle (θ) measurements on a prototype non-polar polyethylene surface, along with Pendant drop tests in order to find out the overall surface tensions (γ) values (Figure 2).

Despite a little fraction of compounds providing polar interactions, bitumen nature is mainly hydrophobic, and its surface free energy is mostly dominated by the dispersive component, related to van der Waals interactions [31]. As RAP is basically aged-bitumen-coated aggregates, a surfactant solution with enhanced values of the surface tension dispersive component, at the expense of lower values of the polar component, results a sensible approach to promote the interaction between MKL emulsifier (stabilizing bitumen emulsion) and bitumen hydrophobic surface. The selection of PE as standard reference for the Sessile drop method is based on its lack of polar component. So, the dispersive component is obtained straightforward with just one test. If the total surface tension of the liquid is previously determined by Pendant drop, the difference between the total and dispersive components gives the polar component.

As shown in Figure 2A, Sessile drop tests were conducted in static mode such that the time-dependent contact angles (θ) were monitored over an image capturing period of 250 s, for all cases studied. It is worth mentioning that evaporation influence was assumed negligible due to the close-saturated system environment employed. For all MKL cases, a sharp decay in contact angle occurs at the beginning of the test, over the first 70s, followed by a milder decrease until steady values were achieved after 250 s.

The Sessile drop test is based on Young equation [32], for a liquid drop on a solid surface, in equilibrium conditions, which can be conveniently arranged as follows:

$$\gamma_L \cdot (1 + cos\theta) \quad = \gamma_S + \gamma_L - \gamma_{S-L} \tag{1}$$

where γ_S, γ_L and $\gamma_{S\text{-}L}$ represent surface tensions (surface free energy) of solid and liquid, and interfacial tension solid-liquid, respectively, and $\gamma_L \cdot (1+\cos\theta)$ is the so-called "adhesion work". Using Owens-Wendt method [33], where the surface tension is calculated as the sum of dispersive (γ^D) and polar (γ^P) components:

$$\gamma = \gamma^D + \gamma^P \tag{2}$$

the adhesion work is expressed as follows:

$$\gamma_L \cdot (1 + cos\theta) = 2\sqrt{\gamma_L^D \cdot \gamma_S^D} + 2\sqrt{\gamma_L^P \cdot \gamma_S^P} \tag{3}$$

For the PE solid used as reference, with only dispersive component of γ_S^D= 35.3 mN/m (literature value), no polar interaction is expected [34]. Thus, by rearranging equation (1) and given that the overall value of surface tension of the liquid (γ_L) is previously determined via pendant drop test, the dispersive contribution of the aqueous phase containing MKL can be obtained by equation (4):

$$\gamma_L^D = \frac{1}{\gamma_S^D}\left[\frac{(1+cos\theta)\cdot\gamma_L}{2}\right]^2 \quad (4)$$

and, then, the liquid polar component is calculated by equation (2).

As previously mentioned, the surface tension (γ) was first obtained from pendant drop technique, which is based on the fact that the curvature of the drop profile is the result of the balance between surface tension and gravitational forces [35]. As observed in Figure 2B, γ value of water (0 wt.% MKL), is 72 mN/m, and gradually decreased down to 59.74 mN/m when concentration of MKL in aqueous phase increases up to 3.75 wt.%, or equivalent to 1.5 wt.% MKL in a 60/40 (O/W) emulsion. The contact angle (θ) on PE substrate (to the right Y axis) decreased sharply from 0 to 0.625 wt.% MKL, and with lower slope between 0.625 to 3.75 wt.% (probably the critical micelle concentration, CMC, has been already attained at 0.625 wt.%). This suggests improved wettability of hydrophobic substrate when MKL is added to the aqueous phase. Moreover, MKL addition altered both dispersive (γ^D) and polar (γ^P) surface tension components. Thus, with the addition of 0.625 wt.% MKL, γ^P is reduced and γ^D is increased.

It is worth noting that the higher the matched ratio of dispersive to polar component between liquid and solid, the more interaction may be expected [33]. Therefore, the effect of the MKL may contribute to improve wetting on bitumen-coated RAP aggregates by the proposed emulsion.

3.2. Processing of bitumen emulsion

Previous results have pointed out the MKL surfactant may affect droplet surface tension, promoting emulsion stabilization mechanisms. Figure 3A presents droplet size distribution (DSD) of 60/40 bitumen emulsions stabilized by 1.5% modified lignin emulsifier, prepared using different emulsification devices. DSD of all emulsions are

fairly similar, except for the one prepared in SilL5M. Apart from emulsification time, study demonstrates that surface weighted or Sauter mean diameter ($D_{3,2}$) values are governed by the dissipation energy [36], that is affected by processing parameters such as rotational speed 'N' where $D_{3,2} \sim N^{-1.2}$ [37]. For emulsions emulsified for a similar time of 4 min, $D_{3,2} \sim N^{-1}$ seems valid, e.g. comparing homogenizers T25 at 20.000 rpm ($D_{3,2(T25\ @20k\ rpm)}$ = 8.5 μm) and SilL5M at 5000 rpm ($D_{3,2(SilL5M\ @5k\ rpm)}$ =26 μm). Nevertheless, $D_{3,2}$ of homogenizer T50 is lower than that of T25, despite emulsion was manufactured with lower N (10000 rpm). In this case, geometry of T50, with larger rotor/stator diameters than T25, also affects $D_{3,2}$ [37]. Thus, both higher rotational speed and larger rotor/stator size increase energy dissipation, which results in the reduction of $D_{3,2}$.

For sake of comparison and scale-up, emulsification was also performed using an in-line homogenizer (3STCM), with a much more robust three-stage-emulsification geometry. As may be seen in Figure 3A and Table 2, DSD and $D_{3,2}$ value obtained were similar to those achieved by the T50 device, although in a shorter emulsification time (1 min or less) and with a larger capacity (Figure 3A). Furthermore, Figure 3B presents DSD curves of 3STCM emulsions stabilized by MKL, for a longer emulsification time up to 12 mins. For comparison, emulsification with the REF emulsifier was also studied. By using 3STCM, emulsification seems sufficient only in one minute of processing, regardless the type of emulsifier. Processing for a longer time does not cause any significant DSD profile change, being average particle size always smaller for REF-stabilized emulsions. By analyzing average mean diameters (calculated from DSD curves) in Table 2, the volume-weighted ($D_{4,3}$) mean diameter seems to be more affected than surface-weighted ($D_{3,2}$) along emulsification time for the MKL-stabilized emulsion.

Flow behavior of emulsions with oil/water (O/W) ratios between 30/70 to 60/40 is shown in Figure 4A. As commonly observed, bitumen emulsion presents shear thinning response at low shear rate, followed by a Newtonian behavior at high shear rate, known as high-shear-rate limiting viscosity (η_∞). As may be seen, η_∞ values are affected by O/W ratio, presenting a higher value as more concentrated bitumen emulsions are, similar results have been already reported elsewhere [38]. All MKL-emulsions show a Newtonian region in a wide shear rate range, even when sheared between 0.1 and 1 s^{-1}. Compared to MKL-emulsions, REF-emulsions present higher shear-thinning character and viscosity for each corresponding O/W ratio, to imply their more highly-structured characteristics as clearly seen under relatively small deformation. Such phenomena might be explained by internal phase fraction, referring to the relation between packing density (ϕ/ϕ_m) a ratio of emulsion volume fraction (ϕ) to its corresponding maximum packing (ϕ_m) and the relative viscosity (η_R). The value of η_R is calculated as the viscosity ratio of emulsion to its continuous phase, and can be fitted as a function of ϕ/ϕ_m by a model for concentrated suspensions, proposed by Frankel-Acrivos (1967), as follows [39]:

$$\eta_R = \frac{\eta_\infty}{\eta_{aqueous\ phase}} = 1.125 \cdot \left[\frac{\left(\frac{\phi}{\phi_m}\right)^{1/3}}{1 - \left(\frac{\phi}{\phi_m}\right)^{1/3}} \right] \quad (5)$$

In Figure 4B, the Frankel-Acrivos fitting curve describes fairly well experimental data. This result suggests η_∞ can be predicted from any O/W ratio higher than 30/70, given that the maximum internal phase value fraction (ϕ_m) is expected to be the same due to relatively similar DSD profiles of each set of emulsions (Figure 3B). In addition, the maximum packing of REF emulsion ($\phi_m = 0.705$) is smaller. Therefore, for a given O/W ratio, their packing density (ϕ/ϕ_m) is always higher than MKL-emulsion. Such densely concentrated systems, governed by the increase in total interfacial area (and, therefore,

by more interactions among droplets), result in more viscous emulsions [40]. On these grounds, the higher Newtonian character and lower viscosity of MKL-stabilized emulsions would favor RAP coating and mixing.

3.3. Reduced-temperature asphalt mixes study

Manufacture of asphalt mixes composed of 100% RAP and fresh bitumen (from previous MKL modified bitumen emulsions), by means of reduced temperature technologies to obtain warm (WMA) and half-warm (HWMA) mix asphalts, will be assessed according to the standards of French design method for hot mixes.

3.3.1 Mix design to meet gyratory and rutting resistance performance specifications

As recommended for a better control of recomposition and homogeneity of the materials [41], RAP (with grading 0/10 mm) was firstly fractioned into four fractions, of 0/2, 2/4, 4/8, and 8/10 mm. After stripping down aged bitumen, obtained fractions were sieved to determine the particle size distribution of their 'cleaned' aggregates (Figure 5A). Then, the quantity of each fraction was adjusted to obtain typical gradation curve for an AC-BBSG 10 design (Figure 5B).

A first approach for mix design, called "white aggregate", fixed the total added bitumen (RAP binder and fresh B160/200) at 5.5% (Table 1) and adjusted the grading curve with fractions 2/4, 4/8, and 8/10 mm, considering the size of cleaned RAP aggregates (Figure 5). Thus, "white aggregate" approach gave rise to the so-called WMA and HWMA mixes, prepared at 130 and 80ºC respectively (Table 1).

The first level of evaluation, according to French design method deals with compactibility performance in French gyratory compactor, as presented in Figure 6. There are several analysis methods to observe the curve of void percentage evolution vs number of gyration. The first study was screened based on the percentage of void (% v/v) at a given

gyrations. The French national foreword of the European standard EN 13108-1 specifies an interval of void values between 5 and 10 % v/v at 60 gyrations for that intended design (AC – BBSG 10). As may be seen in Figure 6 for mixes adapting white aggregate assumption (with the corresponding expected final bitumen content of 5.5%, which is composed of 3.92% RAP binder and 1.6 % of fresh bitumen), WMA reached a 9% void whereas HWMA ("white aggregate") fell beyond expected design value, with 24.4% void.

As an alternative, a semi-quantitative approach, which consisted in adding more fresh bitumen as mixing temperature decreased (Table 1), was proposed. Furthermore, a new grading curve that considered "black aggregate" sizes (coated by RAP binder) and all RAP fractions (from 0/2 to 8/10) was also proposed. This approach based on previous studies [16] that point out a higher blending degree between RAP binder and fresh bitumen in hot mixes asphalt (HMA). However, for reduced-temperature (e.g. WMA and HWMA) asphalt technologies, its blending level is expected to decrease, together with RAP binder quantity able to be rejuvenated, due to the high viscosity of RAP at such low mixing temperatures.

Regarding mix binders, viscous behavior of RAP binder and fresh bitumen were characterized as a function of temperature (Figure 7A). A Newtonian behavior starting from low shear rates, known as zero-shear-rate limiting viscosity (η_0), was always found for both binders, being the aged (harder) bitumen more viscous than the fresh binder. Viscosities decreased with increasing temperature from 60 to 150 °C and were fitted to Arrhenius and WLF models (Equations 6 and 7, respectively):

$$\eta_0(T) = exp\left[\frac{Ea}{R}\left(\frac{1}{T} - \frac{1}{T_0}\right)\right] \quad (6)$$

$$\eta_0(T) = \frac{-C_1(T - T_0)}{[C_2 + (T - T_0)]} \quad (7)$$

where Ea is activation energy, R is universal gas constant, T and T_0 are temperature and its arbitrarily selected reference (90 °C) and C_1 and C_2 are WLF constant. As may be seen in Figure 7B, WLF model, with C_1 and C_2 of 4.9 and 147.1 for fresh bitumen and 9 and 171.8 for RAP binder, fits better than Arrhenius model for viscosity dependence in the whole temperature range studied, from 60 to 150 °C. However, for sake of simplicity and for estimation of fresh bitumen diffusion studied below, Arrhenius equation was used to describe binders viscosity in the mixing temperature range used for WMA and HWMA (80-120 ºC). Thus, Ea will be used for estimating the quantity of fresh bitumen required, based on a thin film diffusion approach. Comparing both bitumen, the higher Ea value of 127 KJ/mol for RAP binder, as compared to fresh bitumen with 80 KJ/mol, suggests a material more susceptible to temperature, arising from a more complex microstructure. Moreover, its higher viscosity and non-Newtonian character are due to the change in chemical composition (i.e. increase in carbonyl and sulfoxide groups, increase molecular association, etc.), which has been associated to long-term aging that leads to a more complex intermolecular interactions within the microstructure [42,43].

Trying to maintain "rejuvenated binder" content similar for both WMA ("white aggregate" approach) and HWMA ("black aggregate") technologies, it is necessary to estimate the amount 'active' RAP binder (i.e. RAP binder layer thickness) available for blending with the fresh bitumen added. Based on the diffusion of fresh bitumen penetrating RAP binder film thickness and a linear relationship between diffusion coefficient and apparent viscosity [17]. The fraction of penetration 'x_T', for a certain depth of aged binder layer coating RAP aggregates, may be estimated for every

temperature of mixing (WMA, HWMA-1 and HWMA-2), with respect to a reference conditions (e.g. Hot Mix Asphalt-HMA processing conditions [16]) as follows,

$$\frac{x_T}{x_{ref}} \approx \left\{ exp\left[\frac{-E_a}{R}\left(\frac{1}{T} - \frac{1}{T_{ref}}\right)\right]\right\}^{0.5} \quad (8)$$

where T_{ref} for a HMA is 150 ºC and x_{ref} takes values between 0.9 and 1 (leading to red and black curves of Figure 8B, respectively), assuming a high partial blending (within the range of 90 to 100% penetration depth) for hot mix asphalt when fresh soft binder is used with RAP [16]. As for Ea value, based on a linear relationship between diffusion coefficient and apparent viscosity [17], diffusion coefficient can be estimated by the Arrhenius equation on diffusion [12, 14, 29, 30] and Ea in Equation 8 could take the value previously calculated for the soft bitumen (Equation 6, Figure 7B). As a result, x_T values calculated for WMA, HWMA-1 and HWMA-2 can be used for estimating RAP binder concentration involved in the diffusion process (Figure 8),

$$\text{“Active” RAP binder (\%)} = x_T \cdot [\text{Total RAP Binder (\%)}] \quad (9)$$

Based on this assumption, the quantity of fresh bitumen, required to maintain the designed binder content, should increase as manufacturing temperature decreases, e.g. by increasing the amount of added MKL-stabilized bitumen emulsion. Thus, Figure 8 estimates about 1.8 % “active” RAP in WMA and Table 1 shows 1.6% fresh bitumen was added, giving 3.4% total binder involved in compaction of the mix. Accordingly, it can be estimated from Figure 8 and Table 1 that 3.4% and 3.6% bitumen (“Active” RAP+B160/220) should be involved in HWMA-1 and HWMA-2, respectively.

Accordingly, both HWMA-1 and HWMA-2 could be sufficiently compacted when black aggregate assumption (or semi-quantitative approach) was used, with design values of 3.4-3.6% total bitumen involved (Figure 6). However, when using “white aggregate”

assumption, mixes prepared at 80 °C (HWMA in Table 1) suffered from poor workability and were unable to be compacted to the expected void percentage (Figure 6). In this case, about 0.20 % "active" RAP is expected to be in HWMA ("white aggregate"), which makes only 1.8% total binder involved in compaction of the mix, when 1.6% fresh bitumen was added (Table 1). Thus, "black aggregate" assumption was proposed for HWMA technology.

Furthermore, analysis of void content at 10 gyrations, that represents the state of materials subjected to low load, was performed to estimate the rutting performance (Figure 6). HWMA-1 presented the lowest value at 13% that suggests a good workability with a drawback of the increasing chance for a poorer rutting performance. In this sense, the rutting resistance was assessed according to EN 12697-22+A1 using wheel tracking device. Figure 9 shows the evolution of deformation depth with the number of cycles. Unfortunately, HWMA-2 ("Black aggregate") specimen for rutting test could not be well-compacted with the common method using a tire roller compactor, likely due to inability for water removal during compaction. Unlike previously used gyratory compactor, in which clean water was observed expelled from the specimen to allow void content at 60 gyrations to be within the specification (Figure 6). For this reason, only WMA and HWMA-1 rutting performance are evaluated in Figure 9. After 30000 cycles, the deformation depths are 5.2 and 8% for WMA and HWMA-1 respectively, which are within specification below the maximum admissible value of 10% for class 1. A higher penetration depth value for HWMA-1 is in agreement with the lowest value of void content after 10 gyrations.

At this point, only two mixes designs, referred to as WMA and HWMA-1, fit the above-mentioned criteria. However, HWMA-2 design will be kept for further assessment with

the aim of validating the proposed semi-quantitative approach and gaining knowledge on mix design for reduced temperature technologies.

3.3.2 Thermo-mechanical and fatigue behaviors

The evolution of the complex modulus (|E*|) and the loss modulus (E") as a function of reduced frequency are presented in Figure 10A. Similar to rutting test preparation, HWMA-2 specimen underwent compaction issues in the tire roller compactor, which resulted in high 13 % void. Nevertheless, trapezoidal specimen for complex modulus and fatigue tests were successfully cut from the slab which is uncommon. Conversely, WMA and HWMA-1 were within the designed void percentage that correlates to the prediction by gyratory test.

According to the French national foreword of EN 13108-1, the norm of the complex modulus (|E*|) at 15 °C and 10 Hz should be either higher than or equivalent to 5500 MPa for AC-BBSG 10 mix class 1 or 7000 MPa for AC-BBSG 10 mix class 2 and 3. |E*| of WMA is 11267 MPa and |E*| of HWMA-1 is 7063 MPa, both satisfying the EN 13108-1 requirement for all classes of AC-BBSG 10. However, the required values are not obtained for HWMA-2 with |E*| of 2492 MPa (Figure 10). The differences in the magnitude among them are likely related to the blended binder properties, which can be estimated for instance by means of technological penetration value (Pen). Thus, by applying logarithmic mixing rule,

$$\log(Pen\_AB) = a \cdot log(Pen_A) + b \cdot log(Pen\_B) \quad (10)$$

where the estimated fraction 'a' of RAP binder (with Pen_A in Table 1) and fresh binder fraction 'b=1-a' (with Pen_B in Table 1) are calculated from Figure 8 and added fresh bitumen from Table 1. By using Equation 10, the blended binder penetrations (Pen_AB) for WMA, HWMA-1 and HWMA-2 are expected to be 40, 99 and 162 dmm, respectively,

assuming “active” RAP binder and total fresh bitumen are fully blended. Therefore, the observed lower modulus |E*| (Figure 10A) and poorer rutting performance (Figure 9) of such mixes may be attributed to a resulting softer binder. Its blend would be composed of less active RAP and more fresh (soft) bitumen, as emulsion-RAP mixing temperature decreases. It is worth noting that LCPC design method advises the use of bitumen with penetrations 35/50 and 50/70 for AC-BBSG-10 [11].

Aiming to further predict mixes behavior for its low temperature performance, a conversion of moduli vs reduced frequency ($a_T \cdot f$) into temperature domain (T) could be performed based on empirical application of time-temperature superposition principle and using a rearranged Arrhenius equation relating shift factor and temperature[44]:

$$T = \frac{Ea \cdot T_{ref}}{R \cdot T_{ref} \cdot \ln(a_T) + Ea} \quad (11)$$

Based on Equation 6 and at a reference temperature of T_{ref}=15 °C, the activation energy is initially obtained by taking the slope of a regression line of ln (a_T) vs T plot (not shown), whose value are 237, 229 and 216 KJ/mol, respectively for WMA, HWMA-1 and HWMA-2. Figure 10B presents the converted master curves into temperature domain. HWMA-1 (and, more apparently, HWMA-2) underwent a shift towards lower temperature in the peak of loss modulus (E”), which has been related to the glassy region onset [45] (Figure 10B). In this regard, a statistically higher fracture temperature is expected as binder becomes harder (i.e. lowering Pen_{25}) [46]. A fact that might be relevant for mix WMA (54% ‘active’ RAP binder and 46% fresh bitumen), which exhibits the highest mechanical glass transition temperature (from E’’ max) at 19 °C. The observed increase in temperature for a given |E*| value as mix binder becomes harder has been reported by other authors [47].

Finally, fatigue resistance was evaluated by means of two-point bending fatigue tests, determining parameter ε_6, a term that represents the strain amplitude to cause the stiffness reduction by half over a million cycles. This value was obtained on a regression line on twelve data points in the logarithmic plot of number of cycles vs deformation (Figure 11). HWMA-2 fatigue life appeared to be quite sensitive to the strain changes, as observed by a steep slope on Nf-ε curve that decreased following sequence HWMA-2, HWMA-1 and WMA. In addition, scattering of data points seemed to narrow along similar sequence. Concerning ε_6 parameter value, the design specification mentions a minimum value of 100 μstrain. Both WMA and HWMA-1 satisfactorily meet the specification, unlike HWMA-2. For a comparative analysis, a correction to ε_6 could be applied for a certain value of compaction degree, which in this case was 7%, using Equation 12 [8,11],

$$\Delta\varepsilon_6 = 3.3 \cdot \Delta(\%v/v) \tag{12}$$

where Δ means the difference between the measured and targeted value for fatigue parameter (ε_6) and void percentage (%v/v). Hence, WMA with 6% and HWMA-1 with 8% have ε_6 corrected value of 103.7 and 107.3 μ_{strain}, respectively. If HWMA-2 were successfully compacted from 13% to 7%, its estimated ε_6 would be 99.8 μstrain which is fairly close the range to satisfy that criteria. Other researchers working on fatigue performance of warm mixes asphalt containing RAP have also reported $\varepsilon_6 > 100$. Dinis-Almeida et al [18], whose work deals with 100% RAP warm mixes within AC 20 grading envelope, presented fatigue performance comparable to their hot mixes at ε_6 of 233, obtained using four point bending technique. For result on two point bending test, Lopes et al [8] also showed that 50% RAP on their warm mixes does not significantly change fatigue performance from their corresponding hot mixes at ε_6 of 115.

Finally, considering a minimum quantity of 5.5% bitumen is required for AC-BBSG-10 design [11], a saving of fresh bitumen by 70 and 50 % could be obtained for WMA and HWMA-1, thus expectedly reduce the impact to environment, in addition to the fact that performance quality meets the specifications.

4. CONCLUDING REMARKS

Asphalt mixes with maximum recycling and minimum impact to environment may be manufactured, between 80 to 130 °C, with a 100 % reclaimed asphalt pavements (RAP) as aggregates and a bitumen emulsion stabilized by modified lignin. The assessment of aqueous phase containing modified lignin suggests that MKL can play roles of emulsion stabilizer along with RAP coating agent. An improved RAP wetting is likely to occur, as may be deduced from its lower contact angle with polyethylene substrate (hydrophobic) compared to water. Regarding its surfactant activity, the surface tension decreases with the increase in concentration from 0 to 0.625% and both polar and dispersive components of surface energy remain constant for higher concentrations.

By using a three-stage in-line homogenizer, the emulsification time shortens below 1 min, since no significant change in $D_{3,2}$ (about 6 μm) is observed for longer times. Compare to reference REF emulsions, MKL-stabilized bitumen emulsions show a lower viscosity, related to their higher maximum packing volume fraction, and a less non-Newtonian character, both factors would favour their use in reduce-temperature asphalt technologies.

Asphalt mixes with 100% RAP may fulfil the French design method when prepared as a WMA or by a HWMA procedure involving the “black aggregate” assumption. HWMA could not be manufactured by the “white aggregate” assumption due to the small amount of fresh bitumen added, which gave rise to a small fraction of activated RAP binder, according to semi quantitative approach. This fact affected mix compatibility.

Conversely, the higher amount of fresh bitumen required by the semi-quantitative method in HWMA-2 led to poor mechanical properties in the mix. In this regard, emulsions formulated with bitumen of lower penetration should be taken into consideration.

Interestingly, a reduction of fresh bitumen content of 70 and 50 % might be expected as reported for WMA and HWMA-1 mixes, respectively, according to minimum binder requirement for a mix AC-BBSG 10. Thus, the semi-quantitative approach becomes relevant in the design of mixes using reduced-temperature method, especially when high rate of recycled asphalt is used. Based on the relation between mixing temperature and fresh bitumen penetration into RAP binder film, a lower manufacturing temperature needs to be compensated by a higher amount of fresh bitumen. Thus, a balance between both parameters should be considered in search of the optimum reduction in lifecycle impact.

5. ACKNOWLEDGEMENTS

This research is a part of the Marie Curie Initial Training Network (ITN) action, FP7-PEOPLE-2013-ITN. This project has received funding from the European Union's Seventh Framework Programme for research, technological development and demonstration under grant agreement number 607524.

6. REFERENCES

[1] B.K. Moon, Overcoming Global Obstacles to Achieve Develpment Goals, in: Achiev. Sustain. Dev. Promot. Dev. Coop., 2008: pp. 9–14. doi:10.2166/wst.2009.028.

[2] M.I. Giani, G. Dotelli, N. Brandini, L. Zampori, Comparative life cycle assessment of asphalt pavements using reclaimed asphalt, warm mix technology and cold in-place recycling, Resour. Conserv. Recycl. 104 (2015) 224–238.

doi:10.1016/j.resconrec.2015.08.006.

[3] D. Lesueur, Polymer modified bitumen emulsions (PMBEs), 2011. doi:10.1016/B978-0-85709-048-5.50002-X.

[4] M. Pérez-Martínez, F. Moreno-Navarro, J. Martín-Marín, C. Ríos-Losada, M.C. Rubio-Gámez, Analysis of cleaner technologies based on waxes and surfactant additives in road construction, J. Clean. Prod. 65 (2014) 374–379. doi:10.1016/J.JCLEPRO.2013.09.012.

[5] M.C. Rubio, F. Moreno, A. Belmonte, A. Menéndez, Reuse of waste material from decorative quartz solid surfacing in the manufacture of hot bituminous mixes, Constr. Build. Mater. 24 (2010) 610–618. doi:10.1016/J.CONBUILDMAT.2009.09.004.

[6] R. Vidal, E. Moliner, G. Martínez, M.C. Rubio, Life cycle assessment of hot mix asphalt and zeolite-based warm mix asphalt with reclaimed asphalt pavement, Resour. Conserv. Recycl. 74 (2013) 101–114. doi:10.1016/j.resconrec.2013.02.018.

[7] A.K. Apeagyei, T.M. Clark, T.M. Rorrer, Stiffness of High-RAP Asphalt Mixtures: Virginia's Experience, J. Mater. Civ. Eng. 25 (2013).

[8] M. Lopes, T. Gabet, L. Bernucci, V. Mouillet, Durability of hot and warm asphalt mixtures containing high rates of reclaimed asphalt at laboratory scale, Mater. Struct. 48 (2015) 3937–3948. doi:10.1617/s11527-014-0454-9.

[9] R.C. West, N.H. Tran, A.J. Taylor, R.J. Willis, Comparison of laboratory cracking test results with field performance of moderate and high RAP content surface mixtures on NCAT test track, in: 8th RILEM Int. Symp. Test. Charact.

Sustain. Innov. Bitum. Mater., 2015: pp. 979–992.

[10] EN13808-8:2005 Bitumen and bituminous binders: Framerwork for specifying cationic bituminous emulsions, n.d.

[11] J.-L. Delorme, C. de la Roche, L. Wendling, LPC Bituminous Mixtures Design Guide, 2007.

[12] M. Zaumanis, R.B. Mallick, R. Frank, 100% recycled hot mix asphalt: A review and analysis, Resour. Conserv. Recycl. 92 (2014) 230–245. doi:http://dx.doi.org/10.1016/j.resconrec.2014.07.007.

[13] D. Lo Presti, A. Jiménez Del Barco Carrión, G. Airey, E. Hajj, Towards 100% recycling of reclaimed asphalt in road surface courses: Binder design methodology and case studies, J. Clean. Prod. 131 (2016) 43–51. doi:10.1016/j.jclepro.2016.05.093.

[14] P. Shirodkar, Y. Mehta, A. Nolan, E. Dubois, D. Reger, L. McCarthy, Development of blending chart for different degrees of blending of RAP binder and virgin binder, Resour. Conserv. Recycl. 73 (2013) 156–161. doi:10.1016/j.resconrec.2013.01.018.

[15] P. Kriz, D.L. Grant, B.A. Veloza, M.J. Gale, A.G. Blahey, J.H. Brownie, R.D. Shirts, S. Maccarrone, Blending and diffusion of reclaimed asphalt pavement and virgin asphalt binders, Road Mater. Pavement Des. 15 (2014) 78–112. doi:10.1080/14680629.2014.927411.

[16] P. Shirodkar, Y. Mehta, A. Nolan, K. Sonpal, A. Norton, C. Tomlinson, E. Dubois, P. Sullivan, R. Sauber, A study to determine the degree of partial blending of reclaimed asphalt pavement (RAP) binder for high RAP hot mix

asphalt, Constr. Build. Mater. 25 (2011) 150–155. doi:10.1016/j.conbuildmat.2010.06.045.

[17] J.W.H. Oliver, Diffusion of Oils in Asphalts, Ind. Eng. Chem. Prod. Res. Dev. 13 (1974) 65–70. doi:10.1021/i360049a013.

[18] M. Dinis-Almeida, J. Castro-Gomes, C. Sangiorgi, S.E. Zoorob, M.L. Afonso, Performance of Warm Mix Recycled Asphalt containing up to 100% RAP, Constr. Build. Mater. 112 (2016) 1–6. doi:10.1016/j.conbuildmat.2016.02.108.

[19] T.M. Slaghek, V.D. Van, C. Giezen, I.K. Haaksman, Bitumen Composition, 2015. Publication number : 20170096558.

[20] S. Laurichesse, L. Avérous, Chemical modification of lignins: Towards biobased polymers, Prog. Polym. Sci. 39 (2014) 1266–1290. doi:10.1016/j.progpolymsci.2013.11.004.

[21] A. Yuliestyan, M. García-morales, E. Moreno, V. Carrera, P. Partal, Assessment of modified lignin cationic emulsifier for bitumen emulsions used in road paving, Mater. Des. 131 (2017) 242–251. doi:10.1016/j.matdes.2017.06.024.

[22] M. Ronald, F.P. Luis, Asphalt emulsions formulation: State-of-the-art and dependency of formulation on emulsions properties, Constr. Build. Mater. 123 (2016) 162–173. doi:10.1016/j.conbuildmat.2016.06.129.

[23] EN1426:2007 Bitumen and bituminous binders. Determination of needle penetration, (n.d.).

[24] EN1427:2007 Bitumen and bituminous binders. Determination of the softening point. Ring and Ball method, n.d.

[25] EN12697-1:2012 Bituminous mixtures. Test methods for hot mix asphalt. Soluble binder content, n.d.

[26] EN12697-3:2013 Bituminous mixtures. Test methods for hot mix asphalt. Bitumen recovery: Rotary evaporator, n.d.

[27] M.. Rodríguez-Valverde, M.. Cabrerizo-Vílchez, P. Rosales-López, A. Páez-Dueñas, R. Hidalgo-Álvarez, Contact angle measurements on two (wood and stone) non-ideal surfaces, Colloids Surfaces A Physicochem. Eng. Asp. 206 (2002) 485–495. doi:10.1016/S0927-7757(02)00054-7.

[28] EN12697-31:2007 Bituminous mixtures. Test methods for hot mix asphalt. Specimen preparation by gyratory compactor, n.d.

[29] EN12697-22:2003 Bituminous mixtures. Test methods for hot mix asphalt. Wheel tracking, n.d.

[30] EN12697-26:2012 Bituminous mixtures. Test methods for hot mix asphalt. Stiffness, n.d.

[31] L. Ziyani, V. Gaudefroy, V. Ferber, F. Hammoum, A predictive and experimental method to assess bitumen emulsion wetting on mineral substrates, Colloids Surfaces A Physicochem. Eng. Asp. 489 (2016) 322–335. doi:10.1016/j.colsurfa.2015.11.002.

[32] S. Wu, Polymer Interface and Adhesion, Marcel Dekker, 1982.

[33] K.L. Mittal, Adhesion and Adhesives: Fundamental and Applied Aspects : Advances in Contact Angle, Wettability and Adhesion, Volume One (1), 2013.

[34] H.W. Starkweather, The surface tension of polyethylene, Polym. Eng. Sci. 5

(1965) 5–6. doi:10.1002/pen.760050102.

[35] C.E. Stauffer, The Measurement of Surface Tension by the Pendant Drop Technique, J. Phys. Chem. 69 (1965) 1933–1938.

[36] J.P. Gingras, L. Fradette, P. Tanguy, E. Jorda, Concentrated bitumen-in-water emulsification in coaxial mixers, Ind. Eng. Chem. Res. 46 (2007) 1818–1825. doi:10.1021/ie061169+.

[37] J.P. Gingras, P.A. Tanguy, S. Mariotti, P. Chaverot, Effect of process parameters on bitumen emulsions, Chem. Eng. Process. Process Intensif. 44 (2005) 979–986. doi:10.1016/j.cep.2005.01.003.

[38] H.A. Barnes, Rheology of emulsions - a review, Colloids Surfaces A Physicochem. Eng. Asp. 91 (1994) 89–95.

[39] N.A. Frankel, A. Acrivos, On viscosity of a concentrated suspension of solid spheres, Chem. Eng. Sci. 22 (1967) 847–853.

[40] Y. Otsubo, R.K. Prud'homme, Flow behavior of oil-in-water emulsions, J. Soc. Rheol. Japan. 20 (1992) 125–131.

[41] C. De la Roche, T. Gabet, M. Van de Ven, W. Van den Bergh, J. Grenfell, Results of interlaboratory tests on a laboratory bituminous mixtures ageing protocol, in: Proceed-Ings 11th Int. Conf. Asph. Pavements, Fr., 2010.

[42] X. Lu, U. Isacsson, Effect of ageing on bitumen chemistry and rheology, Constr. Build. Mater. 16 (2002) 15–22. doi:10.1016/S0950-0618(01)00033-2.

[43] J.F. Masson, T. Price, P. Collins, Dynamics of bitumen fractions by thin-layer chromatography/flame ionization detection, Energy and Fuels. 15 (2001) 955–

960. doi:10.1021/ef0100247.

[44] A.A. Cuadri, M. García-Morales, F.J. Navarro, G.D. Airey, P. Partal, End-performance evaluation of thiourea-modified bituminous binders through viscous flow and linear viscoelasticy testing, Rheol. Acta. 52 (2013) 145–154. doi:10.1007/s00397-012-0671-5.

[45] P. Partal, F. Martınez Bosa, B. Conde, C. Gallegos, Rheological characterisation of synthetic binders and unmodified bitumens, Fuel. 78 (1999) 1–10.

[46] U. Isacsson, H. Zeng, Cracking of asphalt at low temperature as related to bitumen rheology, J. Mater. Sci. 33 (1998) 2165–2170. doi:10.1023/A:1004383506240.

[47] C.F. Quintero Q, L. Momm, L.F.M. Leite, L.L.B. Bernucci, Effect of asphalt binder hardness and temperature on fatigue life and complex modulus of hot mixes, Constr. Build. Mater. 114 (2016) 755–762. doi:10.1016/j.conbuildmat.2016.03.161.

Figure Captions

Figure 1. Process mapping of research methodology.

Figure 2. A) Evolution of contact angle (θ) on polyethylene substrate with respect to time and B) Contact angle (θ), liquid surface tension (γ_L), its disperse component (γ_L^D) and polar component (γ_L^P), of aqueous phase as a function of concentration.

Figure 3. Droplet size distribution of bitumen (160/220) emulsion as a function A) different processing procedure followed (device and emulsification time) and B) effect emulsification time for a selected device three-stage in-line homogenizer - 3STCM.

Figure 4. A) Bitumen emulsion flow curves for O/W ratio within interval range of 60/40 to 30/70 and B) Frankel-Acrivos dependence of relative viscosity with dispersed phase volume fraction for emulsions stabilized by MKL and reference surfactant.

Figure 5. A) Sieve test results of separated RAP fractions (white aggregate), of 0/2, 8/4, 4/8, and 8/10, from which aged binder was previously stripped; and B) their recomposed aggregate gradation referred to AC-BBSG-10 design.

Figure 6. Gyratory compaction performance presenting mix void percentage and number of gyrations.

Figure 7. A) Flow curve of aged binder (extracted from RAP) and bitumen 160/220 (used as raw material for bitumen emulsion) at 60, 90, 120, and 150 °C and B) zero shear-rate limiting viscosity as a function of temperature and their corresponding fitting using Arrhenius and WLF equations.

Figure 8. Semi-quantitative approach for estimating rejuvenated “active” RAP binder as a function of temperature, based on fraction of penetration into the RAP film (x_T) of the fresh bitumen.

Figure 9. Rutting performance at 60 °C (by rut depth) as a function of number of tire-cycles, of 1000, 3000, 10000, and 30000 cycles.

Figure 10. Master curve by applying time-temperature superposition, of A) isothermal plot of moduli vs reduced frequency and B) isochronal plot of moduli vs temperature (obtained by using modified Arrhenius equation).

Figure 11. Fatigue life test by flexion, via two-points bending procedure, and fitting curve of load deformation (μstrain) vs number of cycles (N_F).

Table 1 Asphalt mixes preparation

	White aggregate		Black aggregate	
	WMA	**HWMA**	**HWMA-1**	**HWMA-2**
RAP aggregate				
Temperature °C	130	80	110	80
Binder				
RAP binder (%)	3.92	3.92	4.47	4.47
Additional bitumen (lignin emulsion C60) (%)	1.6	1.6	2.6	3.4
Bitumen emulsion	2.7	2.7	4.3	5.7
Added water (%)	0.75	0.75	0.75	1.5
Processing				
Compaction temp. °C	120	60	90	60

Table 2 Sauter ($D_{3,2}$) and De-Brouckere ($D_{4,3}$) mean diameters of emulsion produced using MKL and REF emulsifier as a function of emulsification time

Emulsification device	**Emulsification time**	**MKL**		**REF**	
		$D_{3,2}$	**$D_{4,3}$**	**$D_{3,2}$**	**$D_{4,3}$**
UT T25	4	8.45	39.04	-	-
UT T50	4	6.01	26.69	-	-
SilL5M	4	25.56	141.26	-	-
3STCM	1	6.70	29.56	2.81	9.66
	2	6.46	28.33	2.68	8.07
	4	5.56	23.31	2.78	12.96
	6	6.63	26.73	2.81	12.19
	10	6.52	25.19	3.03	10.10
	12	6.55	24.92	2.27	5.08

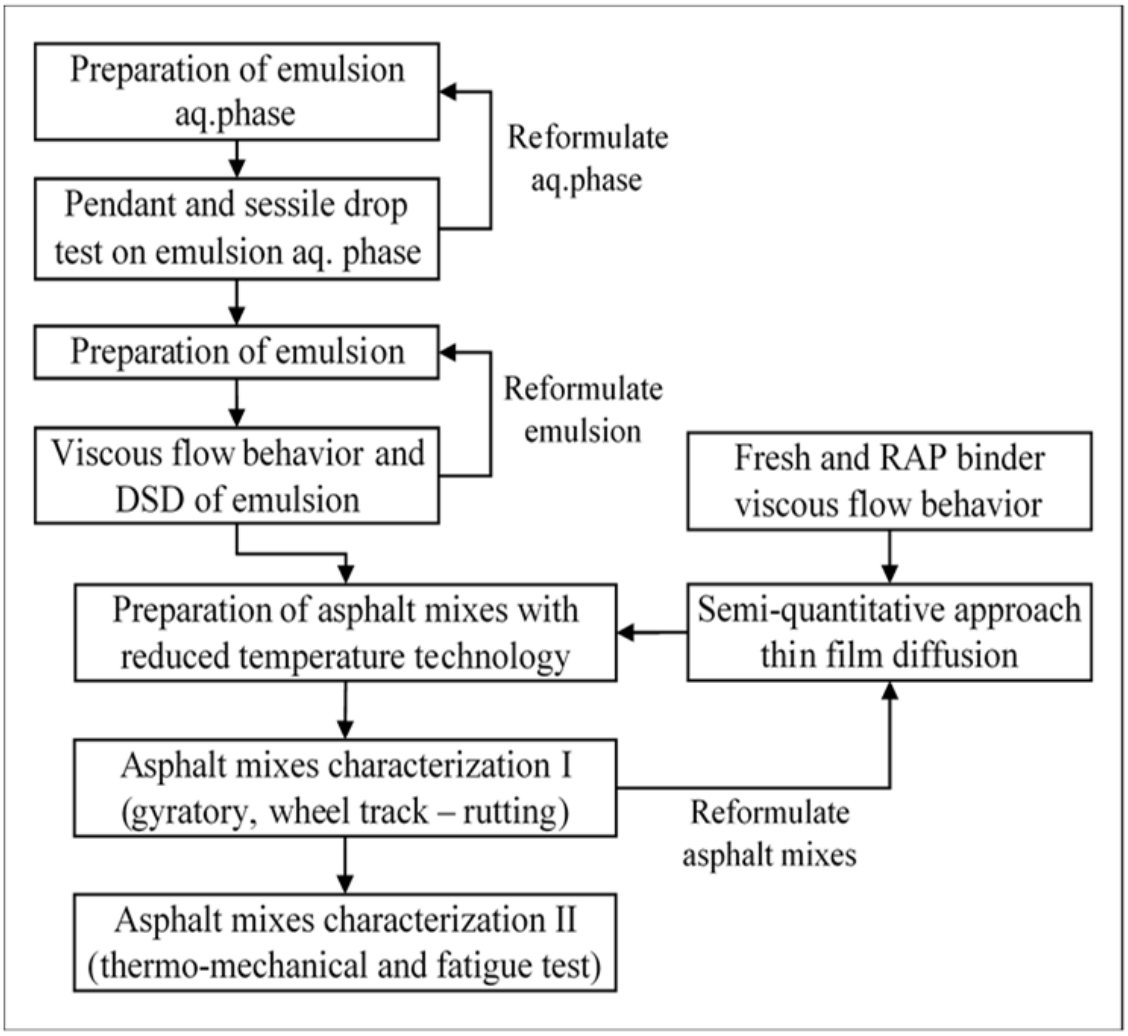
Preparation of emulsion aq.phase
Reformulate aq.phase
Pendant and sessile drop test on emulsion aq. phase
Preparation of emulsion
Reformulate emulsion
Viscous flow behavior and DSD of emulsion
Fresh and RAP binder viscous flow behavior
Preparation of asphalt mixes with reduced temperature technology
Semi-quantitative approach thin film diffusion
Asphalt mixes characterization I (gyratory, wheel track – rutting)
Reformulate asphalt mixes
Asphalt mixes characterization II (thermo-mechanical and fatigue test)

Figure 1

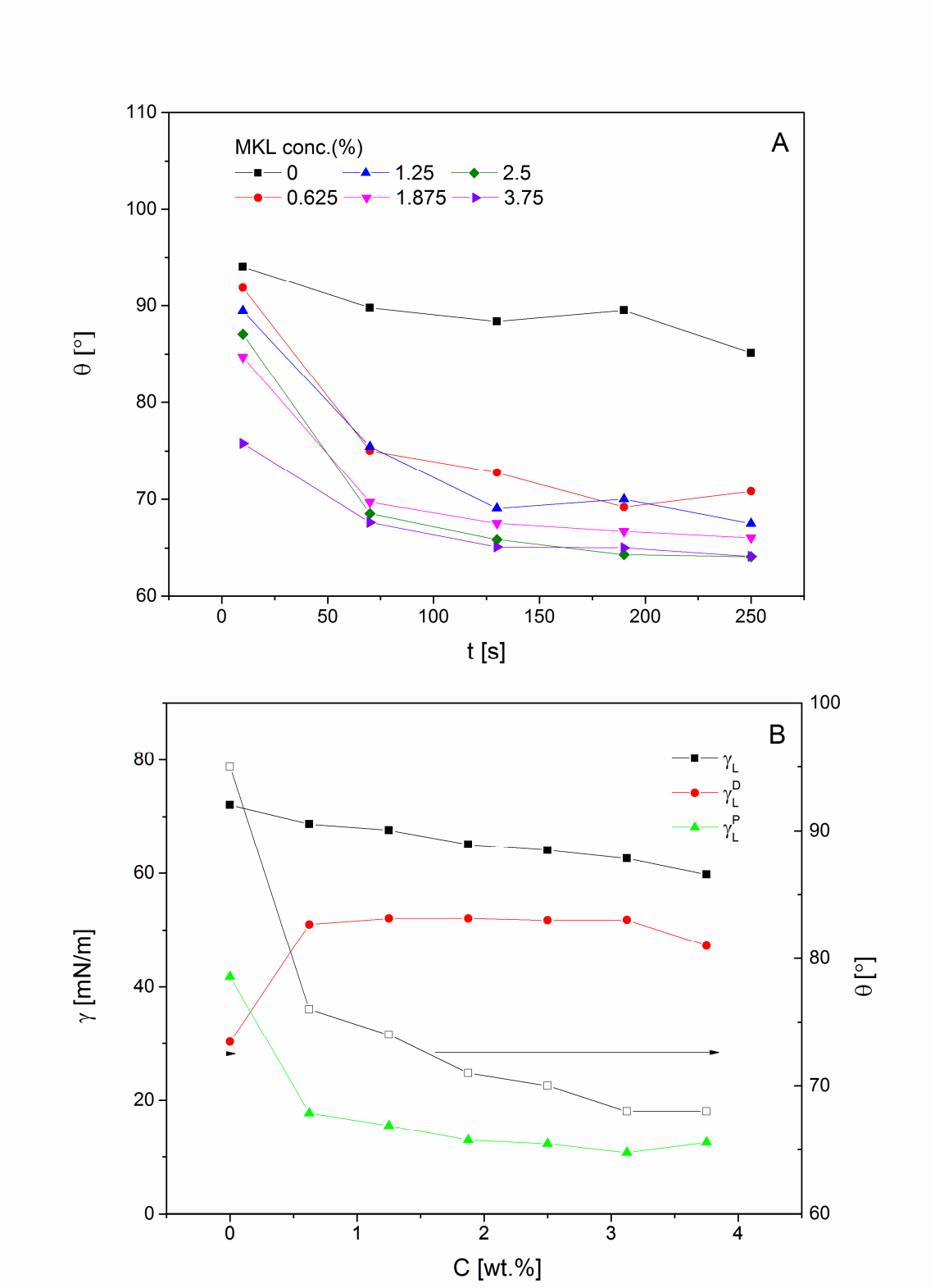

Figure 2

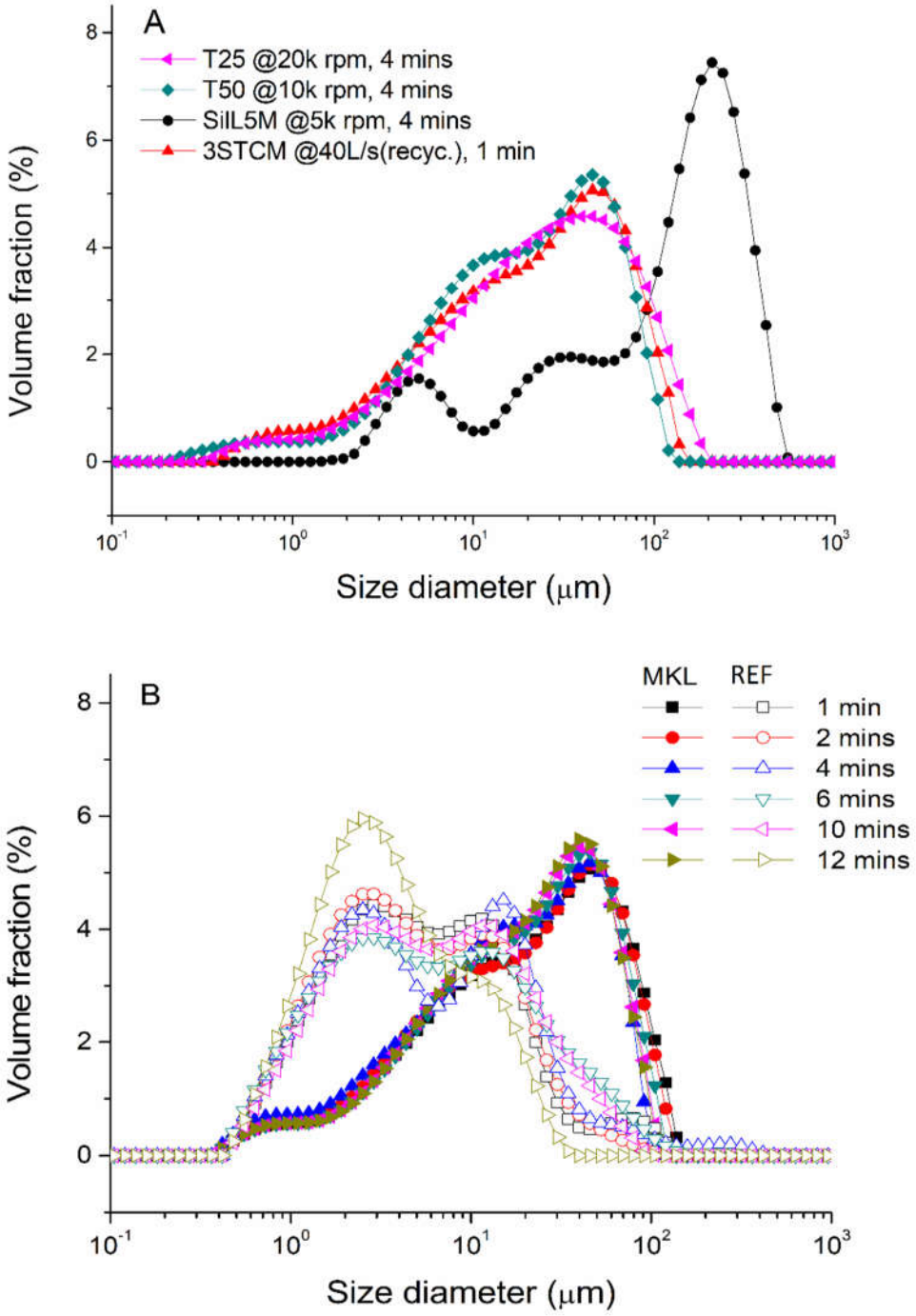
A
T25 @20k rpm, 4 mins
T50 @10k rpm, 4 mins
SilL5M @5k rpm, 4 mins
3STCM @40L/s(recyc.), 1 min
Volume fraction (%)
Size diameter (μm)
B
MKL
REF
1 min
2 mins
4 mins
6 mins
10 mins
12 mins
Volume fraction (%)
Size diameter (μm)

Figure 3

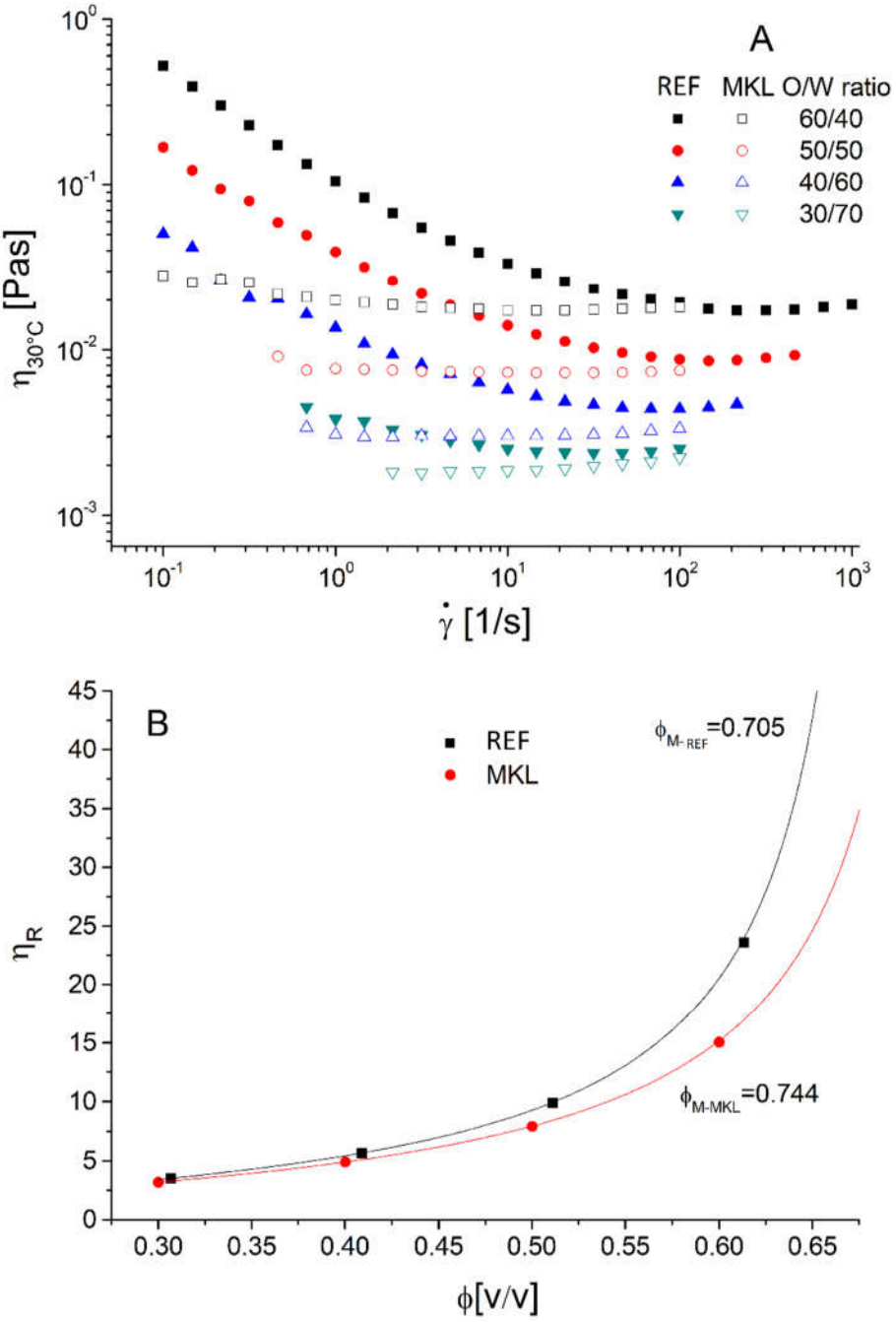
A
REF MKL O/W ratio
60/40
50/50
40/60
30/70
$\eta_{30°C}$ [Pas]
$\dot{\gamma}$ [1/s]
B
REF
MKL
ϕ_{M-REF}=0.705
ϕ_{M-MKL}=0.744
η_R
ϕ[v/v]

Figure 4

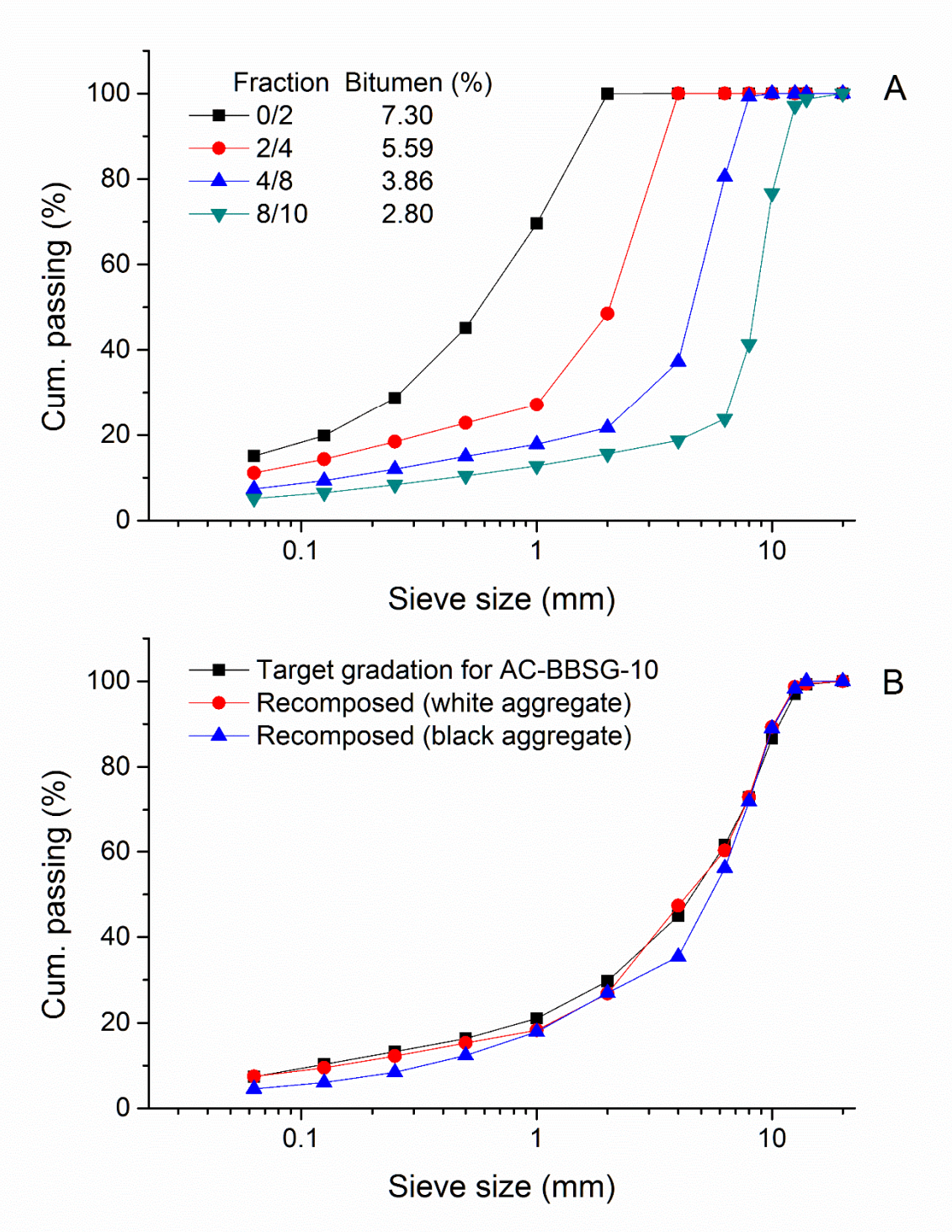
Fraction Bitumen (%)
0/2 7.30
2/4 5.59
4/8 3.86
8/10 2.80
A
Cum. passing (%)
Sieve size (mm)
Target gradation for AC-BBSG-10
Recomposed (white aggregate)
Recomposed (black aggregate)
B
Cum. passing (%)
Sieve size (mm)

Figure 5

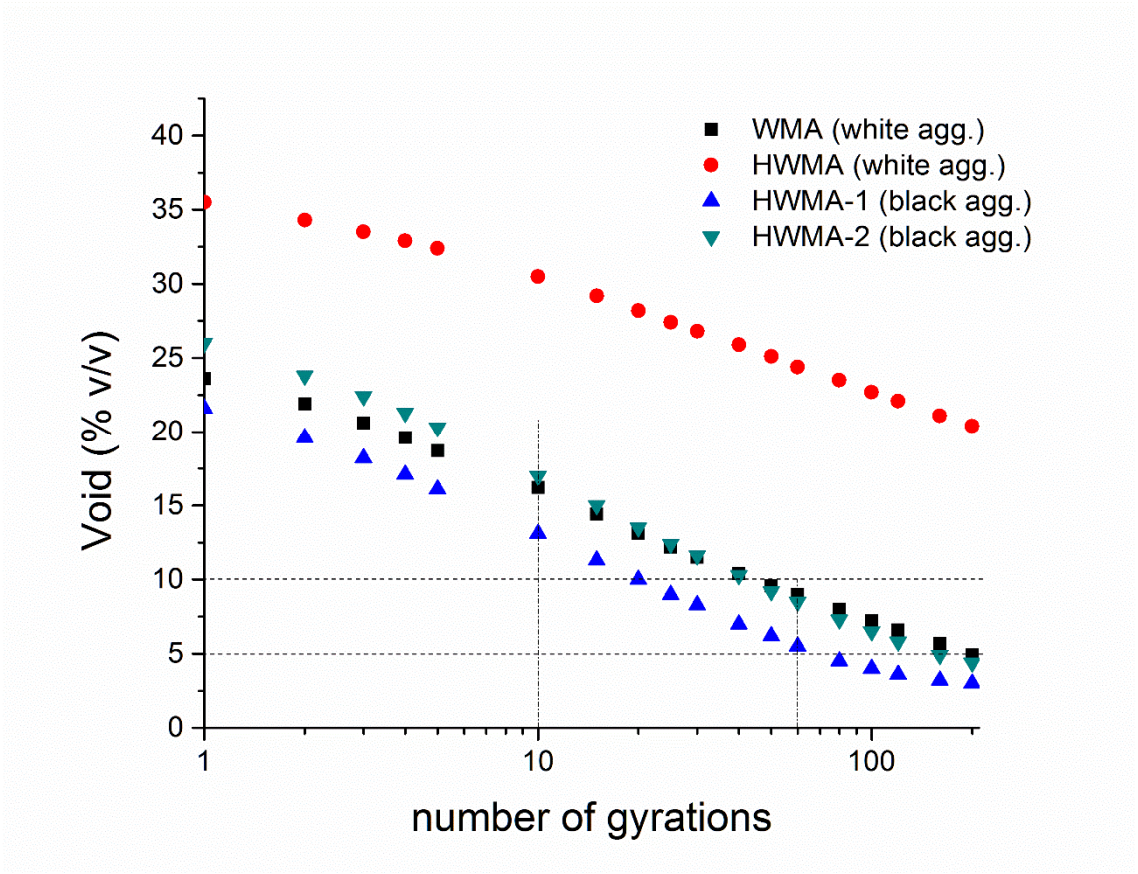
WMA (white agg.)
HWMA (white agg.)
HWMA-1 (black agg.)
HWMA-2 (black agg.)
Void (% v/v)
number of gyrations
0
5
10
15
20
25
30
35
40
1
10
100

Figure 6

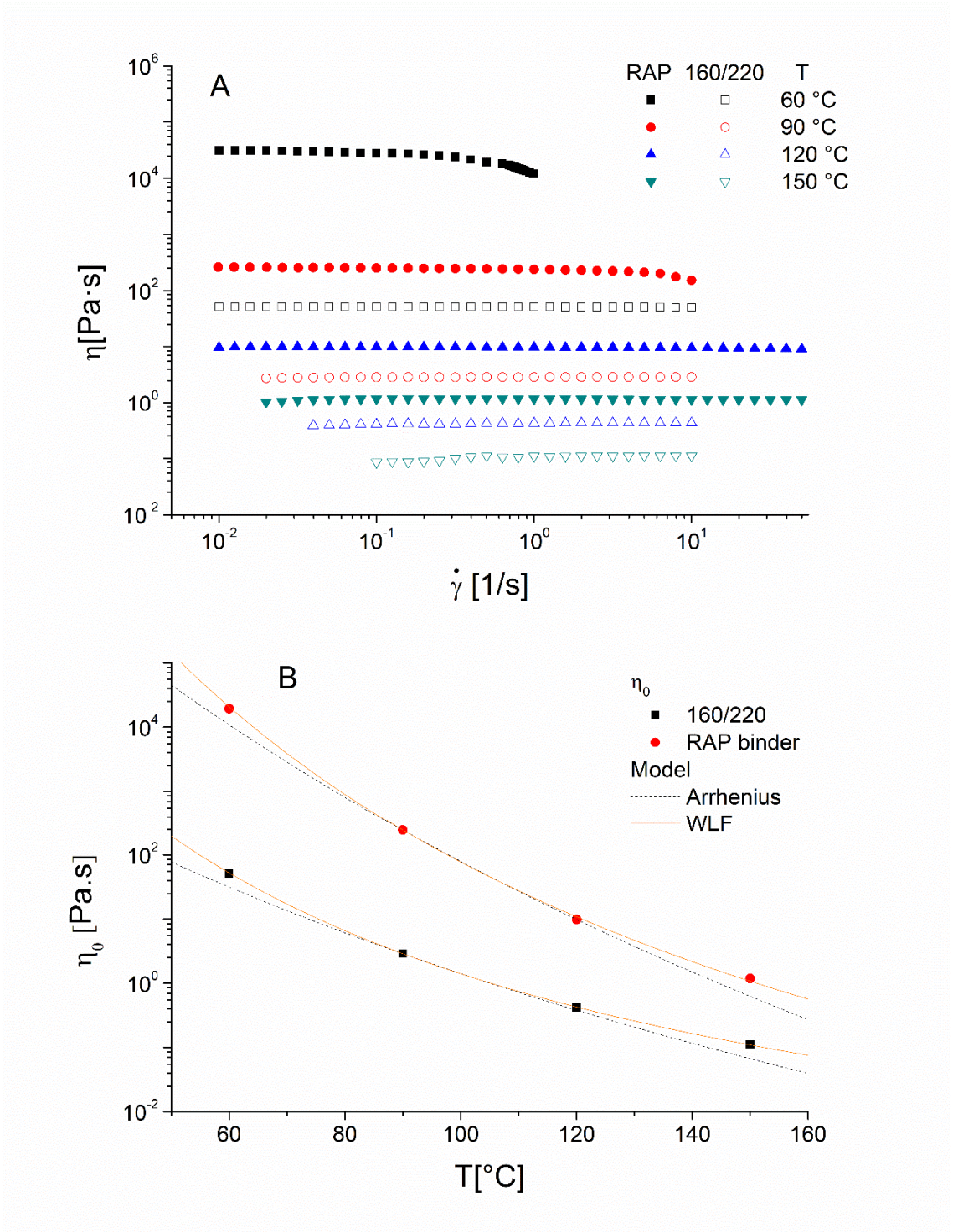
A
RAP 160/220 T
60 °C
90 °C
120 °C
150 °C
η[Pa·s]
$\dot{\gamma}$ [1/s]
B
η0
160/220
RAP binder
Model
Arrhenius
WLF
η0 [Pa.s]
T[°C]

Figure 7

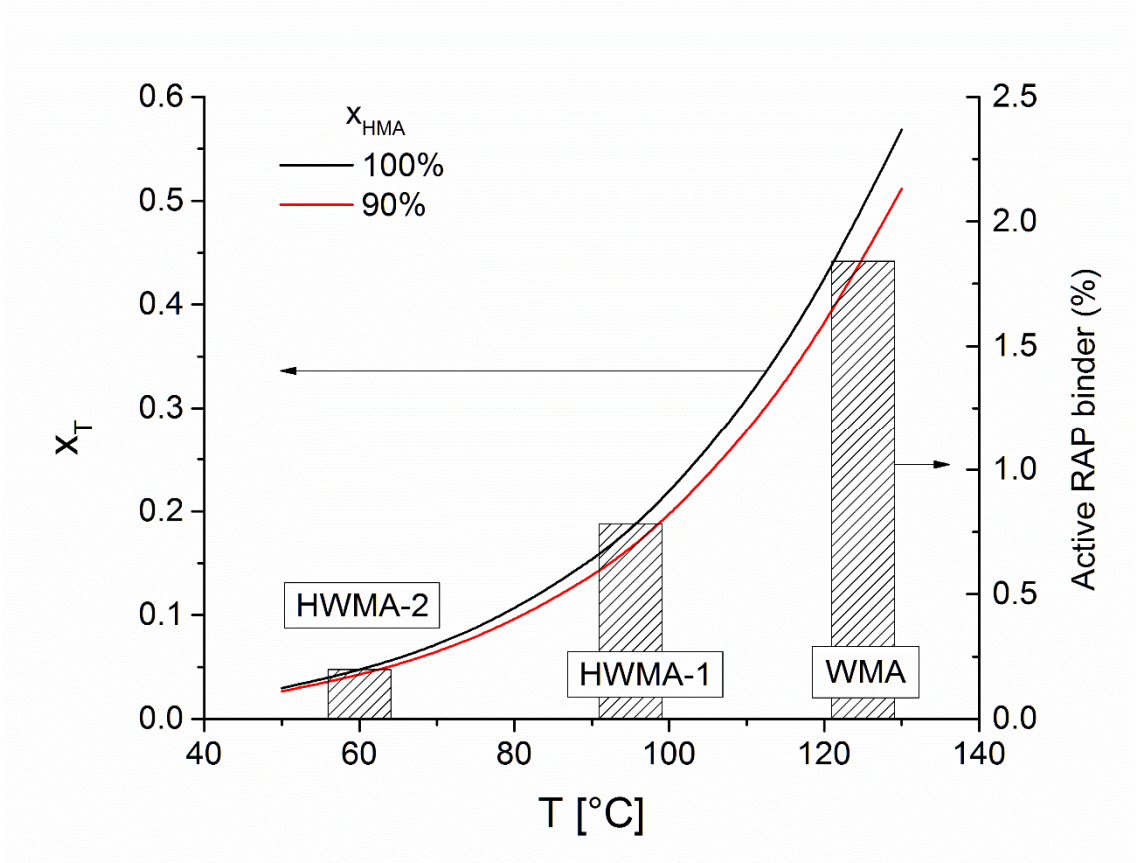
0.6
0.5
0.4
0.3
0.2
0.1
0.0
x_T
x_{HMA}
100%
90%
HWMA-2
HWMA-1
WMA
40
60
80
100
120
140
T [°C]
2.5
2.0
1.5
1.0
0.5
0.0
Active RAP binder (%)

Figure 8

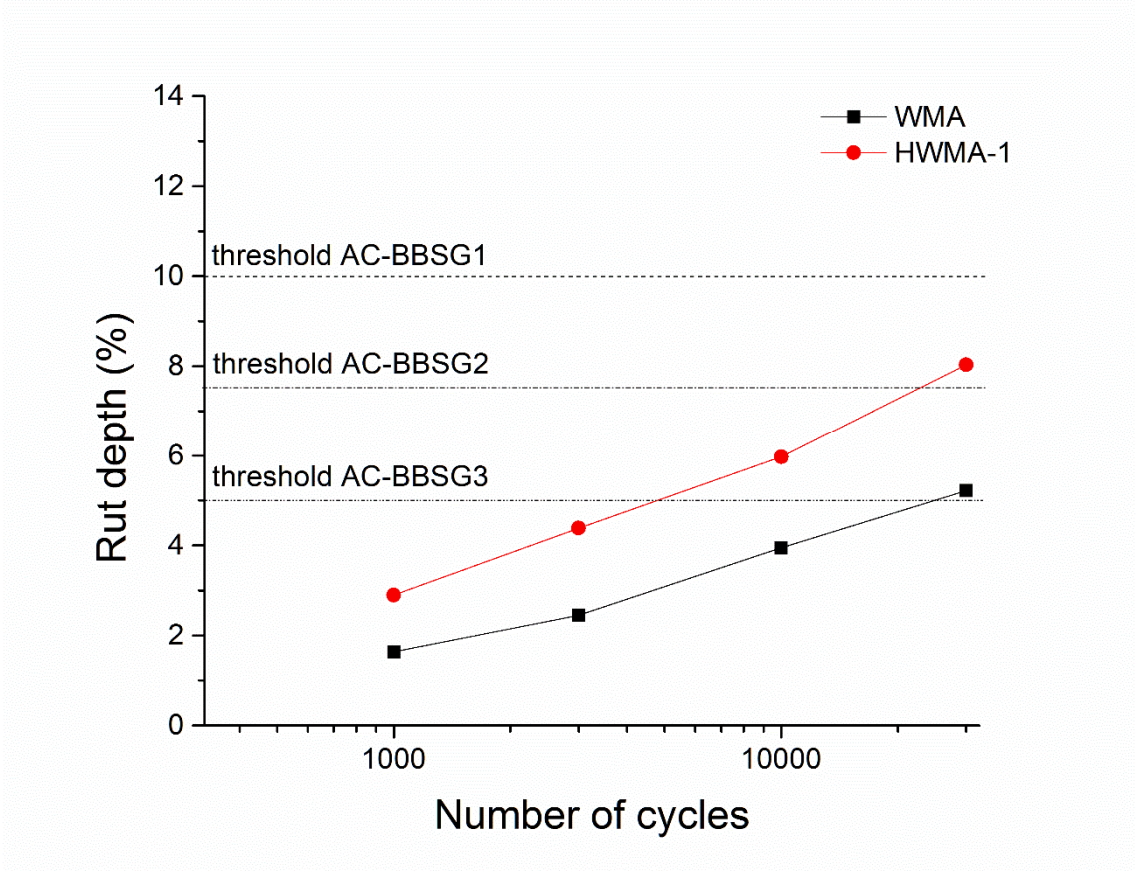
WMA
HWMA-1
threshold AC-BBSG1
threshold AC-BBSG2
threshold AC-BBSG3
Rut depth (%)
Number of cycles
0
2
4
6
8
10
12
14
1000
10000

Figure 9

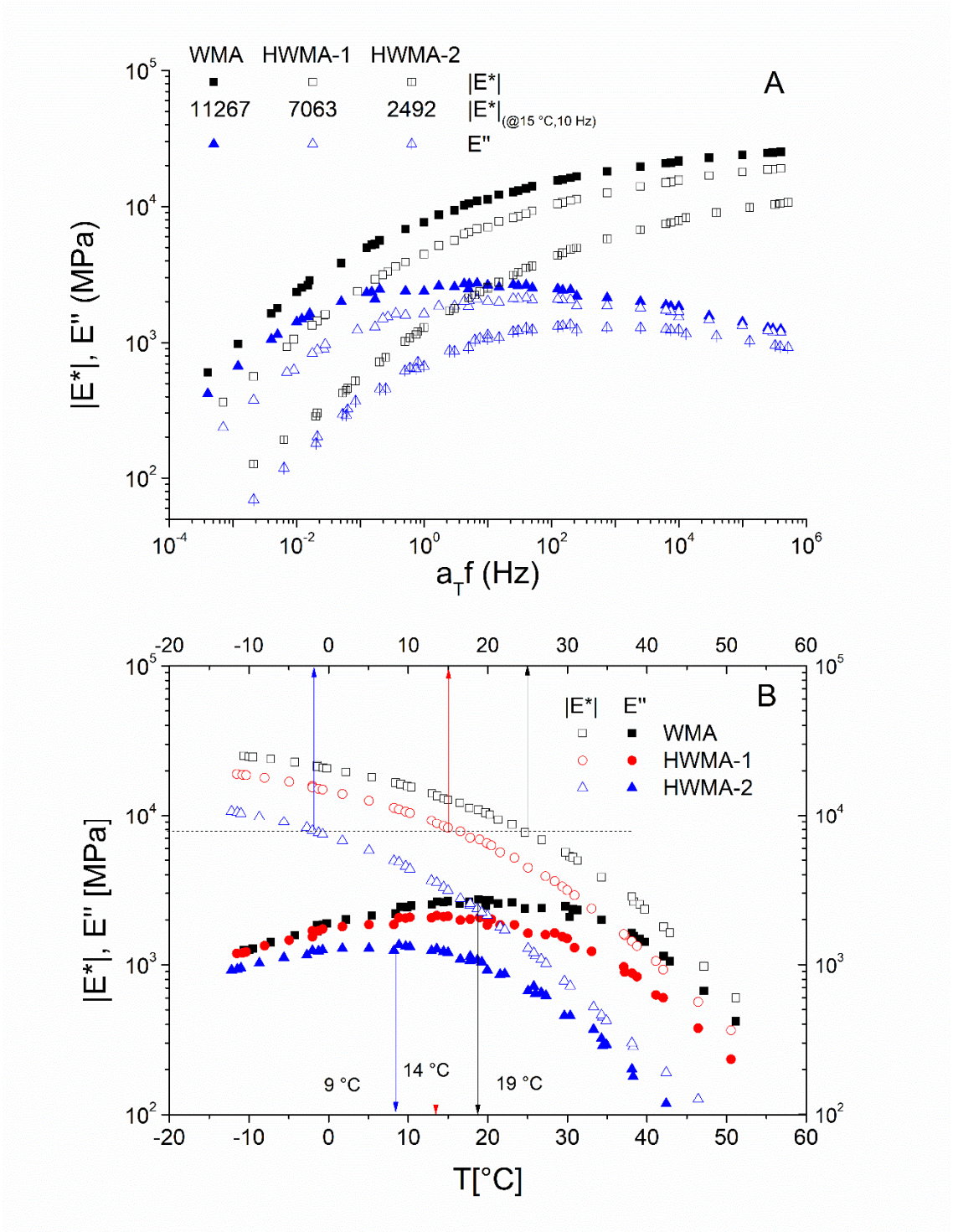
WMA
HWMA-1
HWMA-2
|E*|
11267
7063
2492
|E*|(@15 °C,10 Hz)
E''
A
|E*|, E'' (MPa)
a_T f (Hz)
B
|E*|
E''
WMA
HWMA-1
HWMA-2
9 °C
14 °C
19 °C
|E*|, E'' [MPa]
T[°C]

Figure 10

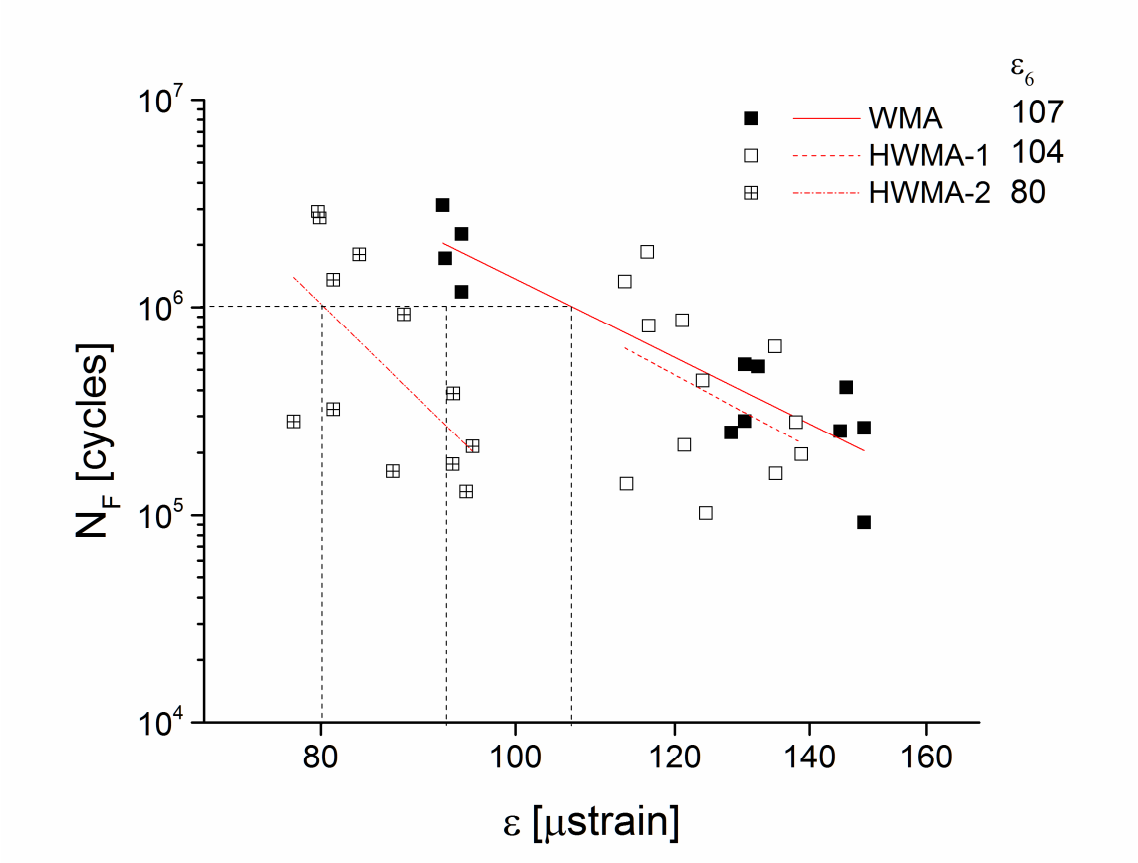
ε_6
WMA 107
HWMA-1 104
HWMA-2 80
10^7
10^6
10^5
10^4
N_F [cycles]
80
100
120
140
160
ε [μstrain]

Figure 11